PROBING FINITE-TEMPERATURE EFFECTS ON ELECTROMAGNETIC DIPOLE TRANSITIONS*

Amandeep Kaur, Nils Paar

Department of Physics, Faculty of Science, University of Zagreb
Bijenička c. 32, 10000 Zagreb, Croatia

Esra Yüksel

Department of Physics, University of Surrey
Guildford, Surrey GU2 7XH, United Kingdom

Received 5 December 2024, accepted 11 December 2024, published online 10 April 2025

We developed a self-consistent finite temperature relativistic quasiparticle random phase approximation (FT-RQRPA) to investigate the behavior of electromagnetic transitions at finite temperature in even–even nuclei. Our investigation focuses on the isotopic chain of $^{40-60}$Ca, exploring the behavior of electric dipole (E1) and magnetic dipole (M1) transitions within a temperature range from $T = 0$ to 2 MeV. The analysis reveals that E1 giant resonance is moderately modified with temperature increase, and new low-energy transitions appear at higher temperatures, making a pronounced impact, particularly in neutron-rich nuclei. This emergence is attributed to the unblocking of transitions above the Fermi level due to thermal effects on single-particle states. Similarly, for M1 transitions, an interesting result is obtained for ^{40,60}Ca nuclei at higher temperatures, *i.e.*, the appearance of M1 transitions, which are forbidden at zero temperature due to fully occupied (or fully vacant) spin–orbit partner states. Furthermore, for Ca isotopes, we observe a shift in M1 strength peaks towards lower energies, primarily attributed to the reduction of spin–orbit splitting energies and residual interactions. The significant temperature dependence observed in the E1 and M1 responses emphasizes their potential importance in the modeling of photon strength functions and their applications in nuclear reaction studies relevant to astrophysics.

DOI:10.5506/APhysPolBSupp.18.2-A4

* Presented at the 57$^{\text{th}}$ Zakopane Conference on Nuclear Physics, *Extremes of the Nuclear Landscape*, Zakopane, Poland, 25 August–1 September, 2024.

1. Introduction

Temperature plays a crucial role in diverse nuclear phenomena, including fusion reactions in stars, nucleosynthesis, and radioactive decay [1]. The impact of finite temperature effects on electromagnetic transitions is evident in a wide range of applications in nuclear physics and astrophysics. Therefore, a precise understanding of electric dipole (E1) and magnetic dipole (M1) transitions under varying temperatures is essential, as these transitions play an important role in various nuclear processes and reactions. In several experimental and theoretical studies, it is highlighted that the low- and high-energy regions of the E1 response get modified at higher temperatures [2–4]. Measuring E1 and M1 transitions in highly excited nuclei presents a significant challenge. Additionally, low-energy dipole transitions near the neutron threshold are crucial for calculating photon-strength functions and astrophysical reaction rates in stellar environments [3, 5].

Various experimental studies on photon-strength functions have revealed intriguing trends, such as a pronounced enhancement in γ-ray strength at lower transition energies, also known as the upbend [4, 6, 7]. While the origin of this upbend behavior remains uncertain, temperature effects can be a plausible factor. These temperature-driven changes in electromagnetic transitions have critical implications for astrophysical phenomena, influencing neutron capture cross sections and the synthesis of elements in stellar environments. Hence, understanding its impact in the low- and high-energy regions of E1 and M1 transitions is of utmost importance.

To study these transitions, various extensions of the random-phase approximation (RPA) based on relativistic and non-relativistic energy density functionals have been employed [3, 8, 9]. These studies consistently reveal the emergence of new excited states, particularly in the low-energy region of the E1 strength, attributed to the thermal unblocking effect on single-particle states near the Fermi level. Recently, the finite temperature extension of fully self-consistent relativistic QRPA (FT-RQRPA) has been established for the studies of E1 and M1 excitations [10, 11]. In the model calculations, we employ a specific class of the relativistic nuclear energy density functional (RNEDF) that includes the point-coupling effective interaction. This class of RNEDFs is particularly convenient due to its simplicity and yields comparable results to those of the meson-exchange effective interactions when describing nuclear ground-state and excited-state properties [12–14]. The objective of this work is to explore the temperature-dependence of isovector E1 and M1 transitions in both the high-energy and low-energy regions for the $^{40-60}$Ca isotopic chain, and to examine their structure in detail.

2. Theoretical framework

A self-consistent finite-temperature relativistic QRPA (FT-RQRPA), based on the RNEDF, has been developed to investigate the effects of temperature on E1 and M1 transitions [10, 11]. The nuclear properties of closed- and open-shell even–even nuclei are described within the finite temperature Hartree–Bardeen–Cooper–Schrieffer (FT-HBCS) framework [15]. The calculations are self-consistent; namely, the same point-coupling interaction, DD-PCX, is used in both the FT-HBCS and FT-RQRPA [14]. The relativistic point-coupling model is formulated in the Lagrangian density,

$$\mathcal{L} = \mathcal{L}_{\mathrm{PC}} + \mathcal{L}_{\mathrm{IV-PV}}\,, \tag{1}$$

where $\mathcal{L}_{\mathrm{PC}}$ includes fermion contact interaction terms as isoscalar–scalar, isoscalar–vector, isovector–vector channels

$$\begin{aligned}\mathcal{L}_{\mathrm{PC}} = {} & \bar{\psi}(i\gamma\,\partial - m)\psi - \frac{1}{2}\alpha_{\mathrm{S}}(\rho)(\bar{\psi}\psi)(\bar{\psi}\psi) - \frac{1}{2}\alpha_{\mathrm{V}}(\rho)\left(\bar{\psi}\gamma^{\mu}\psi\right)\left(\bar{\psi}\gamma_{\mu}\psi\right) \\ & -\frac{1}{2}\alpha_{\mathrm{TV}}(\rho)(\bar{\psi}\vec{\tau}\gamma^{\mu}\psi)(\bar{\psi}\vec{\tau}\gamma_{\mu}\psi) - \frac{1}{2}\delta_{\mathrm{S}}\left(\partial_{\nu}\bar{\psi}\psi\right)\left(\partial^{\nu}\bar{\psi}\psi\right) - e\bar{\psi}\gamma\, A\frac{1-\tau_3}{2}\psi\,.\end{aligned} \tag{2}$$

For the detailed information, see Refs. [14, 16]. The Lagrangian density (1) also includes the relativistic isovector–pseudovector (IV-PV) contact interaction, which is necessary for the FT-RQRPA residual interaction for the unnatural parity excitations of M1 type [17], and is given by

$$\mathcal{L}_{\mathrm{IV-PV}} = -\frac{1}{2}\alpha_{\mathrm{IV-PV}}[\bar{\psi}\gamma^5\gamma^{\mu}\vec{\tau}\psi]\,[\bar{\psi}\gamma^5\gamma_{\mu}\vec{\tau}\psi]\,. \tag{3}$$

The coupling strength parameter $\alpha_{\mathrm{IV-PV}} = 0.63$ MeV fm^3 for DD-PCX parameterization is obtained by minimizing the relative error $\Delta \lesssim 1$ MeV between experimentally determined M1 peak position and theoretically calculated centroid energies for magic nuclei ^{48}Ca and ^{208}Pb [17].

At the finite temperature, the occupation probabilities of single-particle states are given by $n_i = v_i^2(1-f_i) + u_i^2 f_i$, where u_i and v_i are the BCS amplitudes. The temperature-dependent Fermi–Dirac distribution function is defined as $f_i = [1+\exp(E_i/k_{\mathrm{B}}T)]^{-1}$, where T and k_{B} are temperature and Boltzmann constant, respectively. E_i is the quasiparticle (q.p.) energy of a state, calculated as $E_i = \sqrt{(\varepsilon_i - \lambda_q)^2 + \Delta_i^2}$ relation, where ε_i represents the single-particle energies and λ_q denotes chemical potentials for either proton or neutron states. Δ_i indicates the pairing gap of the given state. Note that a separable form of pairing interaction is introduced. The finite temperature

non-charge exchange RQRPA matrix is given by

$$\begin{pmatrix} \widetilde{C} & \widetilde{a} & \widetilde{b} & \widetilde{D} \\ \widetilde{a}^{+} & \widetilde{A} & \widetilde{B} & \widetilde{b}^{\mathrm{T}} \\ -\widetilde{b}^{+} & -\widetilde{B}^{*} & -\widetilde{A}^{*} & -\widetilde{a}^{\mathrm{T}} \\ -\widetilde{D}^{*} & -\widetilde{b}^{*} & -\widetilde{a}^{*} & -\widetilde{C}^{*} \end{pmatrix} \begin{pmatrix} \widetilde{P} \\ \widetilde{X} \\ \widetilde{Y} \\ \widetilde{Q} \end{pmatrix} = E_w \begin{pmatrix} \widetilde{P} \\ \widetilde{X} \\ \widetilde{Y} \\ \widetilde{Q} \end{pmatrix}, \tag{4}$$

where E_w denotes the excitation energies and $\widetilde{P}, \widetilde{X}, \widetilde{Y}, \widetilde{Q}$ are the eigenvectors. The superscript T in Eq. (4) represents the transpose of the matrix elements. Further, the reduced transition probability at finite temperature for E1 and M1 is calculated as described in Refs. [10, 11].

3. Results and discussions

First, we study the isotopic and temperature dependence of low- and high-energy E1 transitions for calcium nuclei. In Fig. 1, the isovector E1 transition strength distributions of $^{40-60}$Ca isotopic chain are shown at temperatures $T = 0$, 0.5, 1, and 2 MeV. On the right side of Fig. 1 [panels (i)–(vi)], the low-energy strength is presented on a logarithmic scale to enhance clarity of the variations occurring in the low-energy region. At $T = 0$ MeV, it is observed that low-energy excited states start to appear, with their strength increasing as the neutron number in Ca isotopes increases. Moreover, low-energy excited states are obtained in the neutron-rich ^{52,56,60}Ca nuclei at energies $E < 12$ MeV, commonly referred to as the pygmy dipole strength.

At low temperatures, *e.g.*, $T = 0.5$ MeV, the dipole strength exhibits minimal change. As the temperature increases to 2 MeV, the high-energy E1 strength redistributes across the main peaks, and the excited states slightly shift towards lower energies, as illustrated in Fig. 1. The temperature effects become increasingly significant in the low-energy region. At $T = 1$ MeV, new low-energy states begin to appear for $E < 12$ MeV. At $T = 2$ MeV, temperature effects become more pronounced in the low-energy region of neutron-rich nuclei, resulting in the emergence of additional low-energy excited states with significant strength. At finite temperatures, the promotion of nucleons to higher energy states alters their occupation probabilities, increasing them above and decreasing them below the Fermi level, thereby broadening the Fermi surface. As a result, thermal unblocking effects become crucial, which enable the new excitation channels, particularly in the low-energy region of the electric dipole response.

Figure 2 shows the M1 transition strength distributions for $^{40-60}$Ca nuclei as a function of increasing temperature. At $T = 0$ MeV, the results for ^{40}Ca ($Z, N = 20$), reveal the absence of any M1 response. This is because the

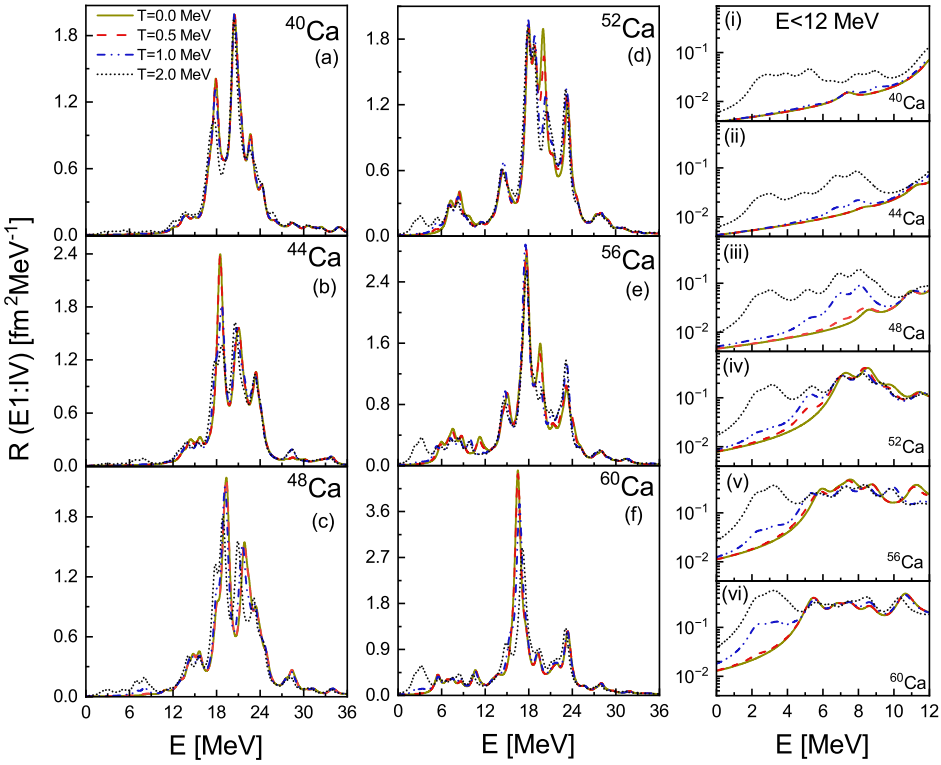

Fig. 1. (Color online) The isovector E1 strength distributions for $^{40-60}$Ca isotopic chain at temperatures from $T = 0$ to 2 MeV [panels (a)–(f)]. The low-energy part of the E1 strength for $E < 12$ MeV is also displayed in logarithmic scale in panels (i)–(vi). Reprinted (figure) with permission from [10]. Copyright (2024) by the American Physical Society.

$(1p_{3/2}, 1p_{1/2})$ and $(1d_{5/2}, 1d_{3/2})$ states are fully occupied for both protons and neutrons, leaving no spin–orbit (SO) partners available for M1 transitions. Similarly, in ^{60}Ca with $N = 40$ neutrons, the states up to $1f_{5/2}$ and $2p_{1/2}$ are fully occupied, prohibiting any M1 transitions. Consequently, no M1 response is observed for these nuclei at zero temperature. For $^{44-56}$Ca, a prominent peak is observed in each isotope, corresponding to the M1 excitation of valence neutron transitions $\nu(1f_{7/2} \rightarrow 1f_{5/2})$. In contrast, M1 transitions for protons are absent due to the shell closure at $Z = 20$. Additionally, a low-energy M1 peak is observed in the ^{52,56}Ca nuclei, attributed to the $\nu(2p_{3/2} \rightarrow 2p_{1/2})$ transition. Further details on the evolution of M1 strength along the $^{40-60}$Ca isotopic chain at zero temperature can be found in Ref. [18].

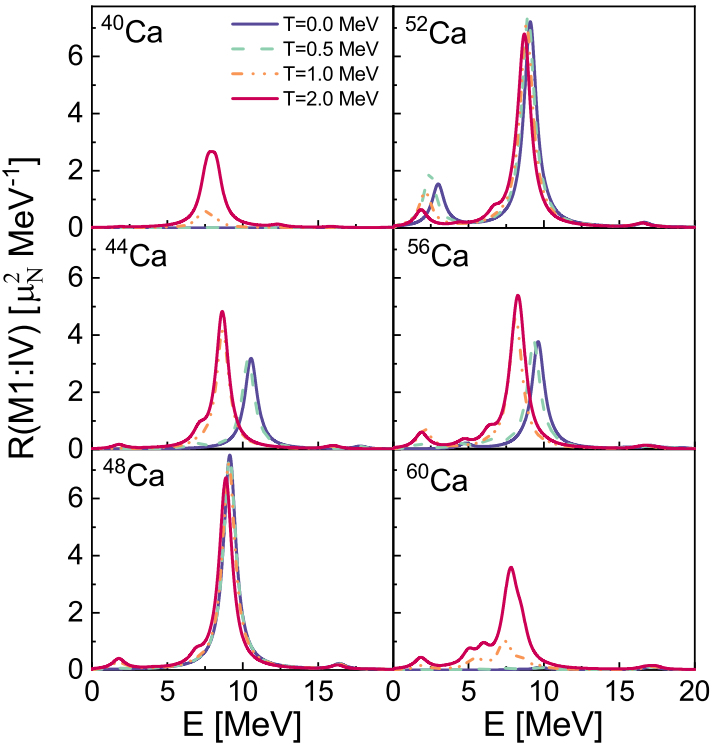

Fig. 2. The isovector M1 strength distributions of $^{40-60}$Ca isotopes calculated using the FT-RQRPA at temperatures from $T = 0$ to 2 MeV. Reprinted (figure) with permission from [11]. Copyright (2024) by the American Physical Society.

As shown in Fig. 2, the M1 transition strength distributions exhibit significant sensitivity to temperature variations. At $T = 0.5$ MeV, the results for Ca isotopes remain largely unchanged. However, with further temperature increases to $T = 1$ and 2 MeV, a notable phenomenon is observed in ^{40}Ca and ^{60}Ca. In these isotopes, M1 transition strength suddenly appears, driven by the emergence of new transitions in the ν, π ($1d_{5/2}$, $1d_{3/2}$) and ν, π ($1f_{7/2}$, $1f_{5/2}$) configurations. This is attributed to temperature-induced particle excitations into higher-energy levels, leading to the thermal unblocking of the previously forbidden M1 transitions. Furthermore, Fig. 2 illustrates a downward shift of up to $\approx$ 2 MeV in the M1 response for ^{44,48,52,56}Ca isotopes as the temperature increases. This behavior is linked to several factors, including reduced pairing correlations in open-shell nuclei, softening of the repulsive residual interaction, and a decrease in spin–orbit (SO) splitting energies with increasing temperature. Thermal unblocking also enables

new proton and neutron transitions, contributing to both the high-energy ($E > 5$ MeV) and low-energy ($E < 5$ MeV) regions of the M1 response in open-shell nuclei ^{44,48,52,56}Ca. In the high-energy region, transitions such as $(1f_{7/2}\rightarrow 1f_{5/2})$ dominate the M1 strength at $T = 1$ and 2 MeV. Additionally, a finite contribution from the $\pi(1d_{5/2}\rightarrow 1d_{3/2})$ transition is observed in $^{40-60}$Ca nuclei at $T = 2$ MeV. In the low-energy region ($E < 5$ MeV), smaller peaks emerge in neutron-rich $^{48-60}$Ca isotopes due to neutron transitions such as $\nu(2p_{3/2}\rightarrow 2p_{1/2})$ and $\nu(1f_{7/2}\rightarrow 1f_{5/2})$. These transitions highlight the role of temperature in reshaping the M1 response across the isotopic chain.

4. Conclusions

A fully self-consistent finite temperature relativistic quasiparticle random phase approximation (FT-RQRPA) framework has been developed to investigate thermal effects on isovector E1 and M1 transitions in the $^{40-60}$Ca isotopic chain. The relativistic density-dependent point-coupling interaction (DD-PCX) is employed in the calculations over a temperature range from $T = 0$ to 2 MeV. The E1 and M1 strength distributions exhibit modifications with increasing temperature, including a shift towards lower energies driven by thermal unblocking effects. Furthermore, new low-energy excitations emerge, especially in neutron-rich isotopes. At higher temperatures, an intriguing phenomenon is observed in ^{40}Ca and ^{60}Ca nuclei: the emergence of M1 excitations that are forbidden at zero temperature due to the complete occupancy or vacancy of spin–orbit partner states. Therefore, the M1 response is shown to be particularly sensitive to temperature variations. These changes are influenced by multiple factors, including the weakening and eventual disappearance of pairing correlations, the softening of the repulsive residual interaction, and the reduction of spin–orbit (SO) splitting energies. The FT-RQRPA framework developed in this work will be further extended in future studies to investigate the evolution of photon strength functions at finite temperatures.

This work is supported by the Croatian Science Foundation under the project Relativistic Nuclear Many-Body Theory in the Multimessenger Observation Era (IP-2022-10-7773). E.Y. acknowledges support from the Science and Technology Facilities Council (UK) through grant ST/Y000013/1.

REFERENCES

[1] K. Langanke, M. Wiescher, *Rep. Prog. Phys.* **64**, 1657 (2001).

[2] H. Wibowo, E. Litvinova, *Phys. Rev. C* **106**, 044304 (2022).

[3] E. Yüksel *et al.*, *Phys. Rev. C* **96**, 024303 (2017).

[4] S. Goriely *et al.*, *Eur. Phys. J. A* **55**, 172 (2019).

[5] A. Bracco, E.G. Lanza, N.S. Martorana, O. Wieland, *Nuovo Cim. C* **47**, 14 (2024).

[6] M. Guttormsen *et al.*, *Phys. Rev. C* **71**, 044307 (2005).

[7] A. Voinov *et al.*, *Phys. Rev. Lett.* **93**, 142504 (2004).

[8] H.M. Sommermann, *Ann. Phys.* **151**, 163 (1983).

[9] Y.F. Niu, N. Paar, D. Vretenar, J. Meng, *Phys. Lett. B* **681**, 315 (2009).

[10] A. Kaur, E. Yüksel, N. Paar, *Phys. Rev. C* **109**, 014314 (2024).

[11] A. Kaur, E. Yüksel, N. Paar, *Phys. Rev. C* **109**, 024305 (2024).

[12] T. Nikšić, D. Vretenar, P. Ring, *Phys. Rev. C* **78**, 034318 (2008).

[13] D. Vale, Y.F. Niu, N. Paar, *Phys. Rev. C* **103**, 064307 (2021).

[14] E. Yüksel, T. Marketin, N. Paar, *Phys. Rev. C* **99**, 034318 (2019).

[15] A.L. Goodman, *Nucl. Phys. A* **352**, 30 (1981).

[16] T. Nikšić, N. Paar, D. Vretenar, P. Ring, *Comput. Phys. Commun.* **185**, 1808 (2014).

[17] G. Kružić, T. Oishi, D. Vale, N. Paar, *Phys. Rev. C* **102**, 044315 (2020).

[18] T. Oishi, G. Kružić, N. Paar, *J. Phys. G: Nucl. Part. Phys.* **47**, 115106 (2020).